Impact of Nonlinearity Including Bleaching in p-i-n Photodetectors on RF-Modulated Electro-Optic Frequency Combs

Seyed Ehsan Jamali Mahabadi , *Student Member, IEEE*, Thomas F. Carruthers, *Senior Member, IEEE*, Curtis R. Menyuk , *Fellow, IEEE*, Jason D. McKinney , *Senior Member, IEEE*, and Keith J. Williams, *Senior Member, IEEE*

Abstract—**We use a drift-diffusion model that includes the effect of bleaching to study the impact of nonlinear distortion in a p-i-n photodetector (PD) on RF-modulated frequency combs. This work complements a similar study that we carried out for a modified uni-traveling carrier (MUTC) PD. We begin by using experimental responsivity data to develop an empirical model of the bleaching in a p-i-n PD when operating in pulsed mode. We then incorporate this model of bleaching into a drift-diffusion model. Next, we use this drift-diffusion model to determine the impact of nonlinearity on the second- and third-order intermodulation distortion products IMD2_n and IMD3_n as a function of the comb line number n. We then determine the corresponding output intercept points OIP2_n and OIP3_n and distortion-to-signal ratios ρ_{2n} and ρ_{3n}. In contrast to MUTC devices, we find that bleaching increases ρ_{2n} and ρ_{3n} at all comb line numbers. However, these distortion products change little as n increases, in contrast to MUTC devices where they grow rapidly as n increases.**

Index Terms—**Photodetector, nonlinearity, frequency combs.**

I. INTRODUCTION

OPTICAL links are an appealing choice for a variety of radio frequency (RF) applications [1]–[2]. Applications include antenna remoting [3], radio-over-fiber [4], beamforming in phased-array radars [5], and optical signal processing of microwave signals [6]. These applications push link lengths towards 100 km or more. For link lengths in this range, stimulated Brillouin scattering [7] (SBS) severely limits the optical launch power, which necessitates the inclusion of either midspan or post-link optical amplification [8]. In many cases (e.g., antenna remoting), midspan amplification is not an option; the use of an amplifier prior to the photodetector drives the link noise figure

substantially above the shot-noise limit [8]. Optical links also have some limitations such as less efficiency, higher noise figure, lower spur-free dynamic range (SFDR), and lower RF power in comparison to purely electronic systems [9].

While any single CW optical signal is limited to powers below the threshold for SBS, additional signals outside the gain bandwidth may be launched into the fiber without penalty. Hence, broadband digital signals are less susceptible to the effects of SBS than are narrowband signals. As each comb line experiences the same RF modulation, the optical comb effectively behaves as an N-element array in the absence of chromatic dispersion as long as the signals are within the detector bandwidth. The RF signals that are recovered from the heterodyne beat of each comb line with its sidebands are coherently summed by the photodetector. Therefore, the comb-based link has the same RF performance as a conventional analog link operating at the same average photocurrent (optical power) level. The important concept here is that the power in each comb line is now limited by the SBS threshold power. Hence, an optical comb with N comb lines can transmit on the order of N times more average power through the link than is possible in a CW laser-based analog link. This approach reduces the dependence on amplification prior to the photodetector in single-span links and may eventually obviate the need for them [8]. This approach has been demonstrated experimentally by McKinney *et al.* [8]

Bleaching or absorption saturation in a high-current photodetector can occur when intense optical fields deplete the number of available final energy states or depopulate the initial states [10]. Additionally, the high density of electrons that is created can increase the possibility that they are recaptured. Regardless of its origin, bleaching leads to a reduction in the photodetector's responsivity as the peak intensity and hence the average power increases. This reduction in responsivity can lead to nonlinear distortion of an incoming RF-photonic signal. Juodawlkis *et al.* [11] have reported that this effect can limit the performance of photonic analog-to-digital converters (PADCs).

Bleaching is an important issue in RF-photonic systems that use frequency combs. Examples include systems that use frequency combs to generate low-noise microwave signals [12] and systems that use frequency combs to disambiguate radar signals [13]. Frequency combs in the RF-domain are generated by using a train of short, high-peak-power optical pulses that

are converted into a comb in the RF-domain by a photodetector. The pulses in a typical optical pulse train have durations less than 500 fs, and are separated by 10–50 ns, corresponding to a repetition rate of 20 MHz to 100 MHz. Hence, the peak power is larger than the average power by a factor of 10^4–10^5.

We calculate the impact of nonlinearity in a p-i-n photodetector (PD) on a frequency comb that is generated by a pulsed optical input. We calculate the impact both with and without bleaching in order to determine the impact of bleaching. The optical input is a train of short optical pulses with a duration of 100 fs and a repetition frequency of $f_r = 50$ MHz that is modulated at microwave frequencies. The PD produces a train of electrical pulses that correspond to a frequency comb in the frequency domain with components at multiples of the repetition frequency. Each comb line is surrounded by components that are separated by the modulation frequencies, as well as intermodulation distortion products that are unwanted in applications [14]–[18].

In previous work, we used experimental data to develop an empirical model of bleaching for both p-i-n and MUTC PDs [14], [15], [18] that we incorporated into the drift-diffusion equations [19]–[21]. In [15], we solved the drift-diffusion equations to determine the impact of nonlinearity in an MUTC PD on a frequency comb. We compared the device nonlinearity both with and without bleaching. The impact of nonlinearity is different for different comb lines. It is standard to characterize the nonlinearity using the second- and third-order intermodulation distortion products, IMD2 and IMD3, as well as the second- and third-order output intercept points, OIP2 and OIP3 [22], [23]. In [15], we defined a separate IMD2_n, IMD3_n, OIP2_n, and OIP3_n for each comb line n, and we used them to characterize the nonlinearity in the MUTC PD. We found that the impact of bleaching on the nonlinearity is complex. The principal effect of bleaching is to lower the responsivity, which also decreases the space charge and lowers the nonlinearity that it induces. This effect is particularly pronounced at comb line numbers n that correspond to large frequencies. The OIP2_n and OIP3_n are always lower with bleaching, but the signal-to-noise ratios $\rho_{2n} = \text{IMD2}_n/S_n$ and $\rho_{3n} = \text{IMD3}_n/S_n$, where S_n is the signal in the n-th comb line, are almost equal at large n. We attribute this result to the reduced space charge when bleaching is present [15].

In this paper, we extend the results to a p-i-n PD with a simple internal structure [19]. As before, we calculate the IMD2_n, IMD3_n, OIP2_n, and OIP3_n for each comb line both with and without bleaching. As was the case for the MUTC PD [15], the OIP2_n and OIP3_n are always lower with bleaching than without. By contrast, the signal-to-noise ratios ρ_{2n} and ρ_{3n} are larger with bleaching than without bleaching for all n, although they converge for large n. Somewhat surprisingly, the nonlinearity is lower for the p-i-n PD than for the MUTC PD at large n. This result differs from our earlier results with the p-i-n and MUTC PDs that operate with a modulated continuous wave (CW) input rather than modulated pulses [19], [21]. We discuss this difference in Sec. 5 of this paper, summarizing an earlier discussion in [14].

The remainder of this paper is organized as follows: In Section II, we review the p-i-n PD structure. In Section III, we
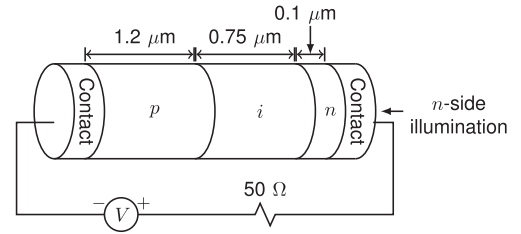

Fig. 1. p-i-n PD structure.

briefly review our bleaching model. In Section IV, we describe the nonlinearity characterization. In Section V, we present our results. Section VI contains the conclusions.

II. p-i-n STRUCTURE

The p-i-n PD structure [24] that we use here is a single heterojunction device made from InP and InGaAs, as shown in Fig. 1. The device is composed of a highly doped transparent n-InP substrate of length $w_n = 0.1$ μm ($N_D = 2 \times 10^{17}$ cm^{-3}), an intrinsic layer of n-InGaAs of length $w_i = 0.75$ μm ($N_B = 5 \times 10^{15}$ cm^{-3}), and a degenerately doped p-InGaAs p-region of length $w_p = 1.2$ μm ($N_A = 7 \times 10^{18}$ cm^{-3}), where N_A and N_D denote the acceptor and donor densities, and N_B denotes the unintentional donor density in the intrinsic region. The total length of the PD is $L = 2.05$ μm. The incident light is assumed to pass through an aperture on the n-side ohmic contact of the device. In the simulation, we set $N_D = 2 \times 10^{17}$ cm^{-3}, $N_A = 7 \times 10^{18}$ cm^{-3}, and $N_B = 5 \times 10^{15}$ cm^{-3}. We modified the length of the intrinsic region from 0.95 μm in the p-i-n structure in [24] to 0.75 μm in order to match the responsivity of the structure in our simulations with experimental data that was collected at the Naval Research Laboratory (NRL). This modification leads to a higher 3-dB bandwidth (29 GHz with 5-V bias) in the modified p-i-n structure than was the case in prior work [24], [25].

III. BLEACHING MODEL

We have developed an empirical model of bleaching, and we incorporated this model into the one-dimensional (1-D) drift-diffusion equations to calculate the responsivity as a function of average input optical power. We modified a model that we previously used [20] to include the effect of bleaching. The details of the model are described in our previous work [15]. The optical generation rate that we use in our drift-diffusion model G_{opt} is given by

$$G_{\text{opt}} = B_f G_c \exp\left[-\alpha(L - x)\right], \qquad (1)$$

where B_f is the bleaching factor, G_c is the generation coefficient without bleaching, α is the absorption coefficient, x is the distance across the device, and L is the device length. This model effectively assumes that the bleaching is instantaneous. That will not be the case in practice, but the finite response time will not affect the model as long as the time for the PD to return to the unbleached state is short compared to the repetition time.

Fig. 2 shows experimental and simulation results of the responsivity of the p-i-n PD as a function of the average input
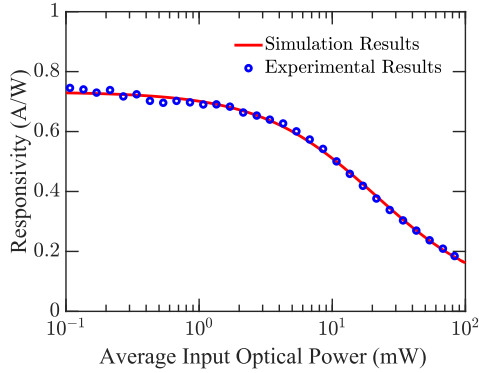
Fig. 2. Responsivity as a function of average input optical power for the p-i-n PD.

optical power with a pulsed input in which pulses have a FWHM duration of 100 fs and a repetition frequency of 50 MHz. The experimental data that we show in Fig. 2 were collected at NRL. In the experiments, a Calmar Mendecino passively-modelocked erbium-doped fiber laser was used. The output of the mode-locked laser was a train of pulses with a 100-fs FWHM pulse duration and a 50-MHz repetition rate. The output was passed through a variable attenuator and a calibrated optical tap with a 90/10 splitter. The 10% tap was used as a power monitor and the 90% tap illuminated the p-i-n PD. The average optical power and average photocurrent were measured as the optical attenuator was adjusted. Knowing the repetition rate, the optical power was then converted to a pulse energy in order to calculate the responsivity [15].

IV. NONLINEARITY CHARACTERIZATION

PD nonlinearity can be measured using one-, two-, and three-tone measurement systems [26]. In our previous work [15] we described the three-tone measurement setup that we are modeling in this study. To model this setup we use

$$P(t) = P_{\text{opt}}(t)$$
$$\{1 + m\left[\sin\left(2\pi f_1 t\right) + \sin\left(2\pi f_2 t\right) + \sin\left(2\pi f_3 t\right)\right]\}, \quad (2)$$

where $P(t)$ is the modulated input optical power, m is modulation depth, f_1, f_2, and f_3 are the three modulation frequencies, and $P_{\text{opt}}(t)$ is the input light power of the optical envelope as a function of time. It is given by

$$P_{\text{opt}}(t) = \sum_n A \operatorname{sech}\left(\frac{t - nT_r}{\tau}\right), \quad (3)$$

where A is the amplitude of input optical power, T_r is the repetition time and τ is the pulse duration. The periodic train of optical pulses corresponds to equally spaced comb lines in the frequency domain that are spaced by the repetition frequency and centered around zero [27]. The output of the PD is a periodic train of electrical pulses that corresponds to comb lines in the frequency domain that are again separated by the repetition frequency. We modulate the input optical pulses with three different frequencies. In our calculations, we used $f_1 = 10$ MHz, $f_2 = 10.5$ MHz, and $f_3 = 9$ MHz. We chose these three frequencies to be close to each other and to fall inside the 50-MHz repetition frequency.

We use a total time window that is 2-μs long and contains an integral number of periods for all three modulation frequencies, so that we avoid aliasing.

We calculate the impact of bleaching on the device nonlinearity as a function of the average input optical power. Second-order intermodulation distortion (IMD2) products and third-order intermodulation distortion (IMD3) products are particularly significant when considering nonlinearity in PDs. The third-order intermodulation products are particularly important because these products can introduce spurious signals that cannot be filtered out from the fundamental response. This is important for microwave photonic (MWP) applications where these would appear as false signals of interest [14]. OIP2 and OIP3 are the key figures of merit to characterize IMD2 and IMD3 [22]. OIP2 and OIP3 are defined as the extrapolated intercept points of the power of the fundamental frequency and the IMD2 and IMD3 powers, respectively. Hence, they characterize the power ratio of the intermodulation products and the fundamental signal. There are second-order intermodulation terms at the frequencies $f_1 \pm f_2$, $f_1 \pm f_3$, and $f_2 \pm f_3$, and third-order intermodulation terms at the frequencies $f_1 + f_2 \pm f_3$ and $f_1 - f_2 \pm f_3$, where f_1, f_2, and f_3 are the modulation frequencies [14].

When studying frequency combs, it is necessary to redefine IMD2, IMD3, OIP2, and OIP3 in a fundamental way. When working in CW mode there is one IMD2, IMD3, OIP2, and OIP3, but when working in pulsed mode, we must determine these quantities for each comb line and IMD2, IMD3, OIP2, and OIP3 become function of comb line number n [14], [15]. We focused on the IMD2$_n$ products at $nf_r + (f_1 - f_2)$ and the IMD3$_n$ products at $nf_r + (f_1 - f_2 + f_3)$. These are the frequency combinations closest to the fundamental frequencies. We calculate one IMD2$_n$ and one IMD3$_n$ and from that one OIP2$_n$ and one OIP3$_n$ for each comb line n. We calculate the IMD2$_n$, IMD3$_n$, OIP2$_n$, and OIP3$_n$ for a single comb line n as a function of comb line frequency $f = nf_r$ where f_r is the repetition frequency of the input optical power (50 MHz) as a function of comb line frequency.

Fig. 3 schematically illustrates the photodetection of a periodic train of three-tone modulated optical pulses, which then produces a train of modulated electrical pulses where $\widetilde{P}_{\text{opt}}(f)$ is the Fourier transform of $P_{\text{opt}}(t)$ and $S(f)$ is the photocurrent spectral density.

V. SIMULATION RESULTS

We calculate the nonlinearity as a function of the average input optical power $P_{\text{opt}}(t)$, given in Eq. 2. For pulsed inputs, we first calculate the impulse response of the PD for different input optical pulse energies, and we then combine the electrical pulse in the time domain, given by 3, taking into account the gap of 20 ns between the pulses, to obtain the total electrical response $P_e(t)$ over a time window of 2 μs [15]. We next calculate the Fourier transform of $P_e(t)$ in order to determine the harmonic powers of the photocurrent for different choices of the amplitude A. Using this approach, along with Eq. 1, we calculate the nonlinear distortion of a pulsed input both with and without bleaching. The principal effect of bleaching is to lower the responsivity of the PD so that fewer electrons are produced.
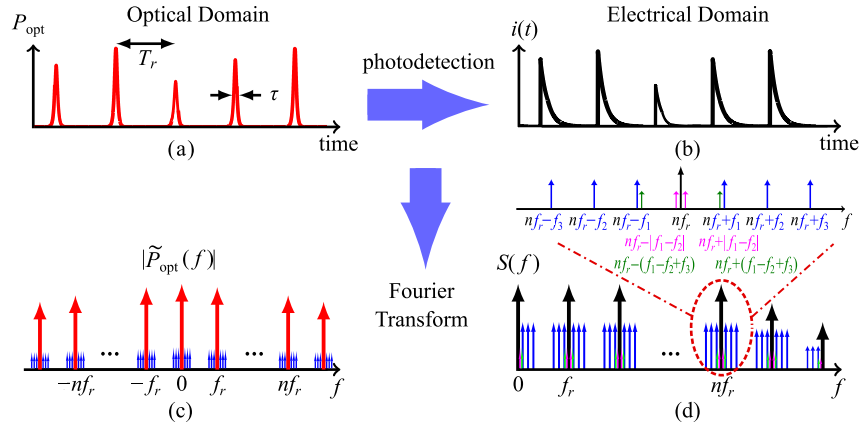
Fig. 3. Time and frequency domain depictions of a modulated optical and photodetected electrical pulse trains, where T_r is the repetition time and τ is the pulse duration of the optical signal. (a) Modulated optical pulse train intensity profile. (b) Modulated photodetected electrical pulse train. (c) Spectrum of the modulated optical intensity profile. (d) Power spectrum of the modulated photocurrent. Adapted with permission from [14] © The Optical Society of America.
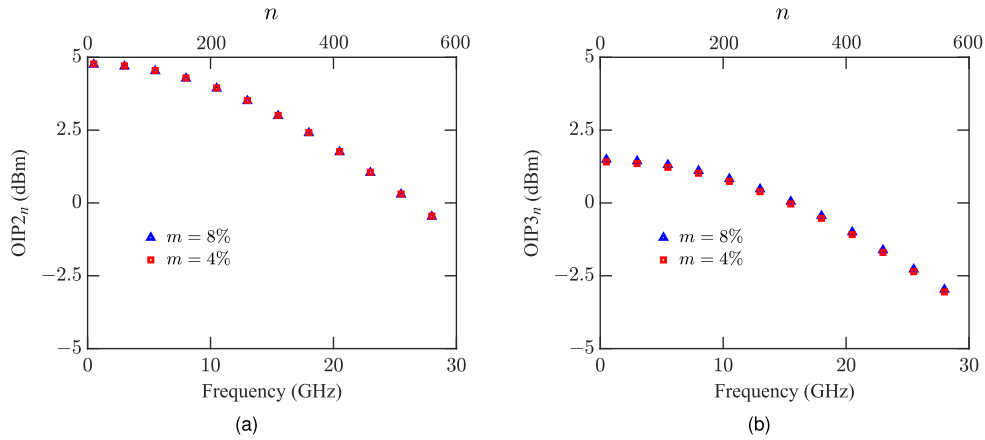

Fig. 4. Comparison of (a) $\mathrm{OIP2}_n$ and (b) $\mathrm{OIP3}_n$ when bleaching is included for $m = 4\%$ and $m = 8\%$ in the p-i-n PD.

That lowers the power at the fundamental frequencies S_n, but also decreases the space charge and hence the nonlinearity, particularly at high frequencies.

Fig. 4 compares $\mathrm{OIP2}_n$ and $\mathrm{OIP3}_n$ for the p-i-n PD with modulation depths $m = 4\%$ and $m = 8\%$ when bleaching is included. As can be seen in Fig. 4, $\mathrm{OIP2}_n$ and $\mathrm{OIP3}_n$ are almost identical for modulation depths $m = 4\%$ and $m = 8\%$. Changing the modulation depth allows us to validate the assumption that we can expand second- and third-order intermodulation distortion powers quadratically and cubically, respectively. We find that this assumption is valid at least up to modulation depth $m = 8\%$, which is also what we found for MUTC PD [15]. All further results will be given for modulation depth $m = 4\%$ since all other results scale appropriately. IMD2 powers scale by the square of the modulation depth and IMD3 powers scale by the cube of the modulation depth up to $m = 8\%$. As a result OIP2 and OIP3 scale linearly/quadratically.

Fig. 5 shows the $\mathrm{OIP2}_n$ and $\mathrm{OIP3}_n$ as a function of frequency at 25 mW average input optical power with and without bleaching for the p-i-n PD. Fig. 5(a) shows the intercept point between the $\mathrm{IMD2}_n$ power and the fundamental power S_n in the n-th comb line, while Fig. 5(b) shows the intercept point between

the $\mathrm{IMD3}_n$ power and the fundamental power S_n. As is the case for the MUTC PDs [15], these intercept points occur at a lower power when bleaching is included than when it is not. The gap is larger for low comb line numbers. The intercept point decreases both with and without bleaching when n increases, but this decrease is noticeably slower when bleaching is included so that the gap is smaller when n is large. By comparing output intercept points in the p-i-n and MUTC PDs when bleaching is included, we found that the $\mathrm{OIP2}_n$ and $\mathrm{OIP3}_n$ for the p-i-n PD have fallen by ~ 5 dB at 28 GHz, while the $\mathrm{OIP2}_n$ and $\mathrm{OIP3}_n$ for the MUTC PD have fallen by more than 20 dB at 18 GHz [14]. This difference is mostly due to the difference in the $\mathrm{IMD2}_n$ and $\mathrm{IMD3}_n$ powers as a function of frequency. The $\mathrm{IMD2}_n$ and $\mathrm{IMD3}_n$ powers both steadily decrease as the frequency increases for the p-i-n PD. By contrast, the $\mathrm{IMD2}_n$ power increases for the MUTC PD up to 10 GHz before starting to decrease, while the $\mathrm{IMD3}_n$ power steadily increases over the entire frequency range [14]. As we discussed in [14], this difference cannot be attributed to the difference in bandwidths between the two devices and is due to the difference in the structures. Fig. 6 shows the separate contribution of the electron current, and hole current, as well as the total current as a function
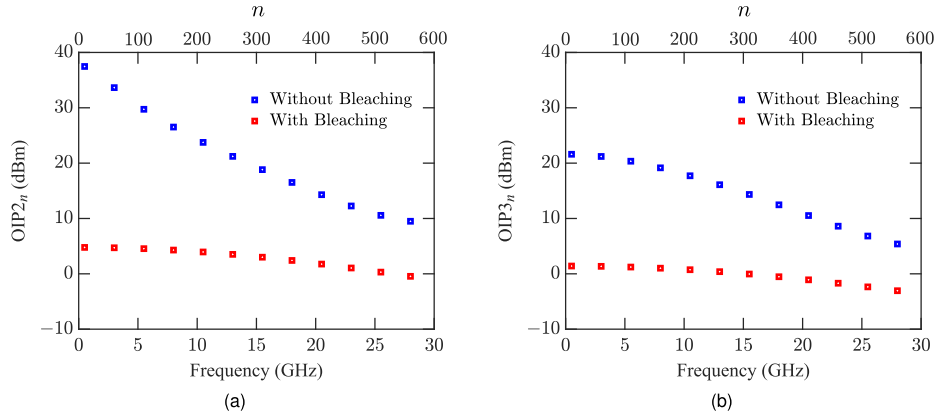
Fig. 5. OIP2_n and OIP3_n as a function of comb line frequency and number for the *p-i-n* PD. (a) OIP2_n. (b) OIP3_n.
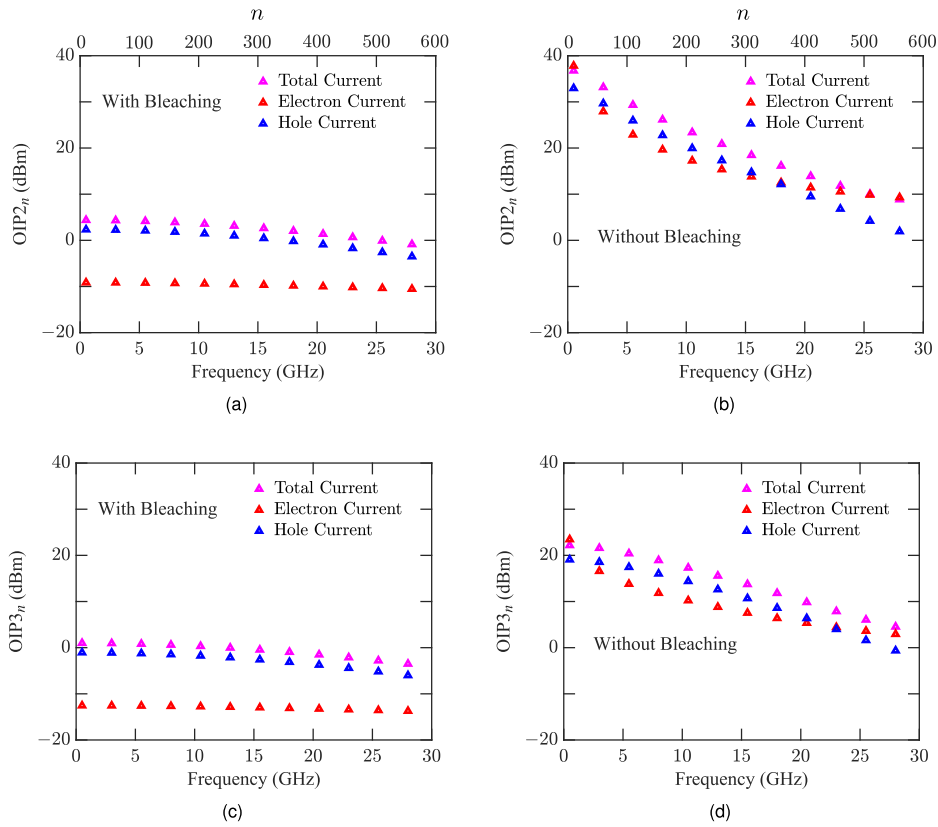

Fig. 6.   Contribution of different current components to OIP2_n and OIP3_n with and without bleaching as a function of comb line frequency and number. The magenta, red, and blue curves show the contributions of the total, electron, and hole currents, respectively. (a) OIP2_n with bleaching, (b) OIP2_n without bleaching, (c) OIP3_n with bleaching, (d) OIP3_n without bleaching.

of comb line frequency to OIP2_n and OIP3_n. The displacement current is more than 40 dB lower than the other currents, and we do not show it. Figs. 6(a) and 6(c) show that the electron current contributes almost 10 dBm less than the hole current to OIP2_n and OIP3_n when bleaching is included. Without bleaching, we find that at comb line frequencies below 2 GHz and beyond 20 GHz, the electron current contributes $\lesssim 5$ dBm more than the hole current, while at comb line frequencies between 2 GHz and 20 GHz the hole current contributes $\lesssim 5$ dBm more than the electron current. These results are consistent with Fig. 3(a) in Ref. [28], in which it is shown that the displacement current does not make a significant contribution to the total current, and

electron and hole currents are the major current components. We also observe that bleaching lowers the electron current more than the hole current, so that the hole current is consistently larger than the electron current.

Fig. 7 shows the fundamental power S_n, the IMD2_n power, and the IMD3_n power for $n = 10\,(nf_r = 0.5\,\text{GHz})$ and $n = 500$ $(nf_r = 25\,\text{GHz})$. In Fig. 7, the dotted curves show the harmonic powers when bleaching is not included and solid curves show the harmonic powers when bleaching is included. Bleaching lowers the fundamental harmonic powers because the responsivity decreases. As shown in Fig. 2, this effect becomes more pronounced as the input optical power increases. For lower
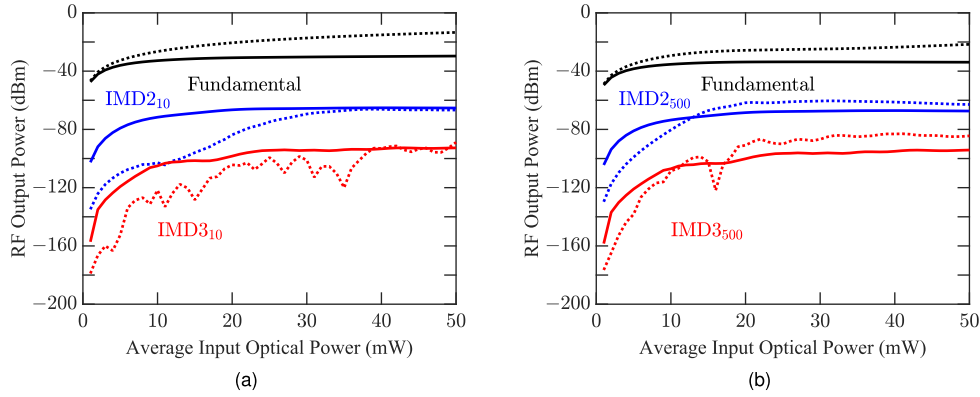
Fig. 7. Power at the fundamental frequency (nf_r), the IMD2_n power at the modulated frequency $nf_r + (f_1 - f_2)$, and the IMD3_n power at the modulated frequency $nf_r + (f_1 - f_2 + f_3)$. Solid lines show results with bleaching; dotted lines show results without bleaching: (a) $n = 10$ $(nf_r = 0.5 \text{ GHz})$, (b) $n = 500$ $(nf_r = 25 \text{ GHz})$.
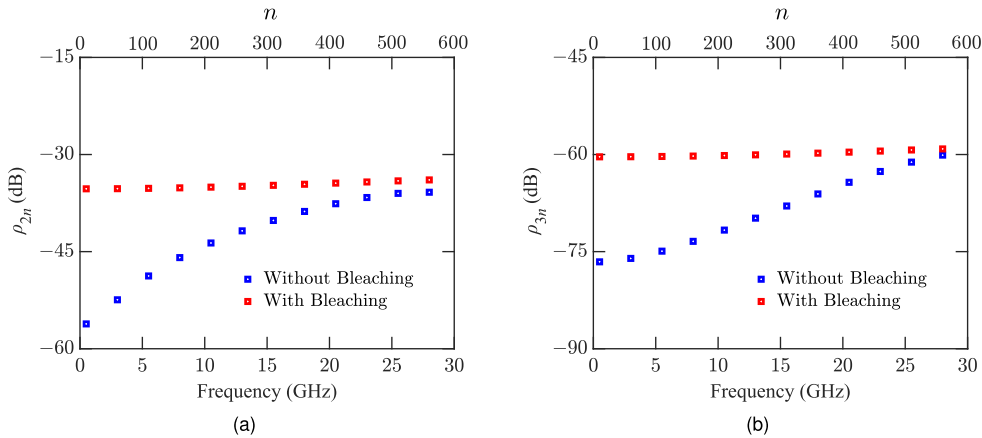

Fig. 8. Signal-to-noise ratios ρ_{2n} and ρ_{3n} as a function of comb line frequency and number for the p-i-n PD. (a) ρ_{2n}. (b) ρ_{3n}.

frequency comb lines, $n \lesssim 100$, we find that the IMD2_n and IMD3_n powers are higher when bleaching is included, but for higher frequency comb lines the IMD2_n and IMD3_n powers are higher when bleaching is not included. When bleaching is included, the frequency domain impulse response falls off less sharply than when it is not included, which we attribute to the reduced space charge. Thus, the impact of bleaching decreases as the comb line frequency increases. We observed a similar effect in the MUTC PD [15].

Fig. 8 shows the distortion-to-signal ratios $\rho_{2n} = \text{IMD2}_n/S_n$ and $\rho_{3n} = \text{IMD3}_n/S_n$ as a function of comb line frequency. Fig. 8 shows that the ratios ρ_{2n} and ρ_{3n} increase as the comb line number increases, but this increase is negligible when bleaching is included. These ratios are higher when bleaching is included than when it is not. The gap decreases as the comb line frequency increases and almost disappears at comb line frequencies beyond 25 GHz. However, in contrast to the MUTC PD [15], bleaching always leads to higher ρ_{2n} and ρ_{3n} up to 28 GHz.

Comparing the behavior of ρ_{2n} and ρ_{3n} in the p-i-n and MUTC PDs as the comb line frequency increases, we previously observed that they increase rapidly for the MUTC PD [14], [15], while Fig. 8 shows that they remain almost constant when bleaching is included. They increase by less

than 3 dB in the p-i-n PD while they increase by more than 12 dB in the MUTC PD. We find that ρ_{2n} is smaller for the p-i-n PD beyond 2 GHz ($n = 40$), while ρ_{3n} is smaller for the p-i-n PD beyond 8 GHz ($n = 160$) when bleaching is included. When bleaching is included, nonlinear distortion has less impact at low frequencies in the MUTC PD than it does in the p-i-n PD, but the opposite is true at higher frequencies [14], [15].

VI. CONCLUSION

We developed an empirical model of bleaching based on experimental data that were collected at the Naval Research Laboratory (NRL), and we incorporated this model into the 1-D drift-diffusion equations to calculate the responsivity. We determined the parameters of the bleaching model in the pulsed mode for the p-i-n PD. We included the bleaching in our drift-diffusion model to study nonlinearity in p-i-n PD in the pulsed mode.

We calculated the impact of bleaching on device nonlinearity as a function of the average optical power. We modeled the three-tone modulation technique to calculate the IMD2 and IMD3 powers in the pulsed mode. We calculated OIP2, and OIP3 to characterize IMD2 and IMD3 and determined the effect of bleaching on the nonlinearity of the p-i-n PD as a function

of average input optical power. The output of modulated optical pulse trains in the PD is a set of frequency comb lines in the frequency domain. By contrast with a CW input, for which there is one IMD2 and one IMD3, each comb line has its own IMD2 and IMD3. We determined the behavior of $IMD2_n$, $IMD3_n$, $OIP2_n$, and $OIP3_n$ for each comb line n with and without bleaching. We found that in the p-i-n PD, $OIP2_n$, and $OIP3_n$ are at a lower power when bleaching is included than when it is not. The difference between the intercepts with and without bleaching is larger for low comb line frequencies. It decreases at high comb line frequencies, and it almost vanishes beyond 25 GHz. $OIP2_n$, and $OIP3_n$ decrease both with and without bleaching when n increases, but this decrease is noticeably slower when bleaching is included. We determined the contribution of electron current, hole current, and displacement current to $OIP2_n$ and $OIP3_n$ in the p-i-n PD. When bleaching is included, we found that displacement current does not make a significant contribution to $OIP2_n$ and $OIP3_n$, and the electron current contributes almost 10 dBm less than the hole current.

We calculated the distortion-to-signal ratios $\rho_{2n} = IMD2_n/S_n$ and $\rho_{3n} = IMD3_n/S_n$ as a function of comb line frequency with and without bleaching. The impact of bleaching on the ratios ρ_{2n} and ρ_{3n} is complex. Its principal effect is to lower the responsivity, which also lowers the space charge. We found that ρ_{2n} and ρ_{3n} increase without bleaching but are almost flat with bleaching. The impact of bleaching diminishes with increasing comb line frequency and almost disappears beyond 25 GHz. The flatness of ρ_{2n} and ρ_{3n} in the p-i-n PD contrast sharply with what we previously found in an MUTC PD [14], [15] in which both ρ_{2n} and ρ_{3n} increase by more than 20 dB over the same frequency range. While nonlinear distortion has more impact on the p-i-n PD than the MUTC PD at low comb line frequencies, the opposite is true at high comb line frequencies.

We conclude that there are two key points for device design. First, while bleaching always makes the nonlinear distortion worse, its impact almost vanishes at high comb line numbers. Hence, bleaching must be taken into account for applications at low frequencies, but is not significant at higher frequencies. Second, in contrast to an MUTC PD, where the impact of nonlinear distortion grows as the comb line number increases, the impact of nonlinear distortion on the p-i-n PD is almost flat, so that the performance eventually exceeds the performance of the MUTC PD as the frequency increases. Hence, the choice of which type device is better depends on the application.

ACKNOWLEDGMENT

REFERENCES

[1] S. E. Jamali Mahabadi, "Modeling phase noise and nonlinearity in photodetectors," Ph.D. dissertation, Univ. Maryland, Baltimore County, MD, USA, 2020.

[2] J. D. McKinney and K. J. Williams, "Sampled analog optical links," *IEEE Trans. Microw. Theory Techn.* vol. 57, no. 8, pp. 2093–2099, Aug. 2009.

[3] A. J. Seeds and K. J. Williams, "Microwave photonics," *J. Lightw. Technol.*, vol. 24, pp. 4628–4641, 2006.

[4] H. Pfrommer *et al.*, "Full-duplex DOCSIS/WirelessDOCSIS fiber-radio network employing packaged AFPM-based base-stations," *IEEE Photon. Technol. Lett.*, vol. 18, no. 2, pp. 406–408, Jan. 2006.

[5] D. Dolfi, D. Mongardien, S. Tonda, M. Schaller, and J. Chazelas, "Photonics for airborne phased array radars," in *Proc. IEEE Int. Conf. Phased Array Syst. Technol.*, 2000, pp. 379–382.

[6] R. A. Minasian, "Photonic signal processing of microwave signals," *IEEE Trans. Microw. Theory Techn.*, vol. 54, no. 2, pp. 832–846, Feb. 2006.

[7] G. P. Agrawal, *Nonlinear Fiber Optics*. Boston, MA, USA: Academic, 1995.

[8] J. D. McKinney, V. J. Urick, and J. Briguglio "Optical comb sources for high dynamic-range single-span long-haul analog optical links," *IEEE Trans. Microw. Theory Techn.*, vol. 59, no. 12, pp. 3249–3257, Dec. 2011.

[9] C. H. Cox, E. I. Ackerman, G. E. Betts, and J. L. Prince, "Limits on the performance of RF-over-fiber links and their impact on device design," *IEEE Trans. Microw. Theory Techn.*, vol. 54, no. 2, pp. 906–920, Feb. 2006.

[10] V. J. Urick, Keith J. Williams, and Jason D. McKinney, *Fundamentals of Microwave Photonics*. Hoboken, NJ, USA: Wiley, 2015.

[11] P. W. Juodawlkis *et al.*, "Absorption saturation nonlinearity in InGaAs/InP p-i-n photodiodes," in *Proc. 15th Annu. Meeting IEEE Lasers Electro Opt. Soc.*, 2002, pp. 426–427.

[12] J. Millo *et al.*, "Ultra-low-noise microwave extraction from fiber-based optical frequency comb," *Opt. Lett.*, vol. 34, pp. 3707–3709, 2009.

[13] S. R. Harmon and J. D. McKinney, "Broadband RF disambiguation in subsampled analog optical links via intentionally-introduced sampling jitter," *Opt. Exp.*, vol. 22, pp. 23928–23937, 2014.

[14] S. E. Jamali Mahabadi, T. F. Carruthers, C. R. Menyuk, J. D. McKinney, and K. J. Williams, "Comparison of the impact of nonlinearity in a and an MUTC photodetector on electro-optic frequency combs," *Opt. Lett.*, vol. 46, pp. 813–816, 2021.

[15] S. E. Jamali Mahabadi, T. F. Carruthers, C. R. Menyuk, J. D. McKinney, and K. J. Williams, "Impact of nonlinearity including bleaching in MUTC photodetectors on RF-modulated electro-optic frequency combs," *Opt. Exp.* vol. 29, pp. 11520–11532, 2021.

[16] S. E. Jamali Mahabadi, T. F. Carruthers, C. R. Menyuk, M. N. Hutchinson, J. D. McKinney, and K. J. Williams, "Impact of nonlinearity on RF-modulated frequency combs with different modulation depths in an MUTC photodetector," in *Proc. IEEE Int. Topical Meeting Microw. Photon.*, 2019, pp. 1–4.

[17] S. E. Jamali Mahabadi, T. F. Carruthers, C. R. Menyuk, M. N. Hutchinson, J. D. McKinney, and K. J. Williams, "Impact of nonlinearity in an MUTC photodetector on an RF-modulated frequency comb," in *Proc. IEEE Photon. Conf.*, 2019, pp. 1–2.

[18] S. E. Jamali Mahabadi, T. F. Carruthers, C. R. Menyuk, J. D. McKinney, and K. J. Williams, "Impact on frequency combs of nonlinearity including bleaching in photodetectors," in *Proc. IEEE Photon. Soc. Summer Topicals Meeting Ser.*, 2020, pp. 1–2.

[19] Y. Hu, B. S. Marks, C. R. Menyuk, V. J. Urick, and K. J. Williams, "Modeling sources of nonlinearity in a simple p-i-n photodetector," *J. Lightw. Technol.* vol. 32, pp. 3710–3720, 2014.

[20] Y. Hu, "Modeling nonlinearity and noise in high-current photodetectors," Ph.D. dissertation, Univ. Maryland, Baltimore County, MD, USA, 2017.

[21] Y. Hu, C. R. Menyuk, M. N. Hutchinson, V. J. Urick, and K. J. Williams, "Frequency dependent harmonic powers in a modified uni-traveling carrier photodetector," *Opt. Lett.* vol. 42, pp. 919–922, 2017.

[22] D. M. Pozar, *Microwave Engineering*. Hoboken, NJ, USA: Wiley, 2009.

[23] K. J. Williams, R. D. Esman, and M. Dagenais, "Nonlinearities in p-i-n microwave photodetectors," *J. Lightw. Technol.* vol. 14, pp. 84–96, 1996.

[24] M. N. Draa, A. S. Hastings, and K. J. Williams, "Comparison of photodiode nonlinearity measurement systems," *Opt. Exp.*, vol. 19, pp. 12635–12645, 2011.

[25] F. Quinlan, T. M. Fortier, H. Jiang, and S. A. Diddams, "Analysis of shot noise in the detection of ultrashort optical pulse trains," *J. Opt. Soc. Amer. B*, vol. 30, pp. 1775–1785, 2013.

[26] S. E. Jamali Mahabadi and C. R. Menyuk, "Calculation of the impulse response of PIN and MUTC photodetectors using the drift-diffusion equations," presented at the Meeting, Laser Sci. Washington, DC, USA, 2017, Paper JTu 2A-53.